

1-1-2012

Properties of the B⁺-H₂ and B⁺-D₂ complexes: a theoretical and spectroscopic study

B L. J Poad
University of Wollongong, bpoad@uow.edu.au


V Dryza
University of Melbourne

A A. Buchachenko
Moscow State University

J Kos
University of Maryland

E J. Bieske
University of Melbourne

Follow this and additional works at: <https://ro.uow.edu.au/scipapers>

 Part of the [Life Sciences Commons](#), [Physical Sciences and Mathematics Commons](#), and the [Social and Behavioral Sciences Commons](#)

Recommended Citation

Poad, B L. J; Dryza, V; Buchachenko, A A.; Kos, J; and Bieske, E J.: Properties of the B⁺-H₂ and B⁺-D₂ complexes: a theoretical and spectroscopic study 2012.
<https://ro.uow.edu.au/scipapers/4764>

Properties of the B⁺-H₂ and B⁺-D₂ complexes: a theoretical and spectroscopic study

Abstract

The rotationally resolved infrared spectrum of the B⁺-D₂ ion-neutral complex is recorded in the D-D stretch vibration region (2805–2875 cm⁻¹) by detecting B⁺ photofragments. Analysis of the spectrum confirms a T-shaped equilibrium geometry for the B⁺-D₂ complex with a vibrationally averaged intermolecular bond length of 2.247 Å, around 0.02 Å shorter than for the previously characterised B⁺-H₂ complex [V. Dryza, B. L. J. Poad, and E. J. Bieske, *J. Am. Chem. Soc.* 130, 12986 (2008)10.1021/ja8018302]. The D-D stretch band centre occurs at 2839.76 ± 0.10 cm⁻¹, representing a -153.8 cm⁻¹ shift from the Q₁(0) transition of the free D₂ molecule. A new three dimensional ab initio potential energy surface for the B⁺⁺-H₂ interaction is calculated using the coupled cluster RCCSD(T) method and is used in variational calculations for the rovibrational energies of B⁺-H₂ and B⁺-D₂. The calculations predict dissociation energies of 1254 cm⁻¹ for B⁺-H₂ with respect to the B⁺⁺-H₂ (j = 0) limit, and 1313 cm⁻¹ for B⁺-D₂ with respect to the B⁺⁺-D₂ (j = 0) limit. The theoretical approach reproduces the rotational and centrifugal constants of the B⁺-H₂ and B⁺-D₂ complexes to within 3%, and the magnitude of the contraction of the intermolecular bond accompanying excitation of the H₂ or D₂ sub-unit, but underestimates the H-H and D-D vibrational band shifts by 7%–8%. Combining the theoretical and experimental results allows a new, more accurate estimation for the B⁺-H₂ band origin (3939.64 ± 0.10 cm⁻¹).

Keywords

complexes, theoretical, spectroscopic, study, b, properties, d2, h2

Disciplines

Life Sciences | Physical Sciences and Mathematics | Social and Behavioral Sciences

Publication Details

Poad, B. L. J., Dryza, V., Buchachenko, A. A., Kos, J. & Bieske, E. J. (2012). Properties of the B⁺-H₂ and B⁺-D₂ complexes: a theoretical and spectroscopic study. *Journal of Chemical Physics*, 137 (12), 124312-1-124312-8.

Properties of the B⁺-H₂ and B⁺-D₂ complexes: A theoretical and spectroscopic study

B. L. J. Poad, V. Dryza, A. A. Buchachenko, J. Kłos, and E. J. Bieske

Citation: *J. Chem. Phys.* **137**, 124312 (2012); doi: 10.1063/1.4754131

View online: <http://dx.doi.org/10.1063/1.4754131>

View Table of Contents: <http://jcp.aip.org/resource/1/JCPSA6/v137/i12>

Published by the [American Institute of Physics](#).

Additional information on *J. Chem. Phys.*

Journal Homepage: <http://jcp.aip.org/>

Journal Information: http://jcp.aip.org/about/about_the_journal

Top downloads: http://jcp.aip.org/features/most_downloaded

Information for Authors: <http://jcp.aip.org/authors>

ADVERTISEMENT



Goodfellow
metals • ceramics • polymers • composites
70,000 products
450 different materials
small quantities fast

www.goodfellowusa.com

Properties of the B^+-H_2 and B^+-D_2 complexes: A theoretical and spectroscopic study

B. L. J. Poad,^{1,a)} V. Dryza,¹ A. A. Buchachenko,^{2,3,b)} J. Kłos,^{4,c)} and E. J. Bieske^{1,d)}

¹School of Chemistry, The University of Melbourne, Parkville, VIC 3010, Australia

²Department of Chemistry, M. V. Lomonosov Moscow State University, Moscow 119991, Russia

³Institute of Problems of Chemical Physics RAS, Chernogolovka, Moscow District 142432, Russia

⁴Department of Chemistry and Biochemistry, University of Maryland, College Park, Maryland 20742-2021, USA

(Received 16 July 2012; accepted 27 August 2012; published online 28 September 2012)

The rotationally resolved infrared spectrum of the B^+-D_2 ion-neutral complex is recorded in the D-D stretch vibration region (2805–2875 cm^{-1}) by detecting B^+ photofragments. Analysis of the spectrum confirms a T-shaped equilibrium geometry for the B^+-D_2 complex with a vibrationally averaged intermolecular bond length of 2.247 Å, around 0.02 Å shorter than for the previously characterised B^+-H_2 complex [V. Dryza, B. L. J. Poad, and E. J. Bieske, *J. Am. Chem. Soc.* **130**, 12986 (2008)]. The D-D stretch band centre occurs at $2839.76 \pm 0.10 \text{ cm}^{-1}$, representing a -153.8 cm^{-1} shift from the $Q_1(0)$ transition of the free D_2 molecule. A new three dimensional *ab initio* potential energy surface for the B^+-H_2 interaction is calculated using the coupled cluster RCCSD(T) method and is used in variational calculations for the rovibrational energies of B^+-H_2 and B^+-D_2 . The calculations predict dissociation energies of 1254 cm^{-1} for B^+-H_2 with respect to the B^++H_2 ($j = 0$) limit, and 1313 cm^{-1} for B^+-D_2 with respect to the B^++D_2 ($j = 0$) limit. The theoretical approach reproduces the rotational and centrifugal constants of the B^+-H_2 and B^+-D_2 complexes to within 3%, and the magnitude of the contraction of the intermolecular bond accompanying excitation of the H_2 or D_2 sub-unit, but underestimates the H-H and D-D vibrational band shifts by 7%–8%. Combining the theoretical and experimental results allows a new, more accurate estimation for the B^+-H_2 band origin ($3939.64 \pm 0.10 \text{ cm}^{-1}$). © 2012 American Institute of Physics. [<http://dx.doi.org/10.1063/1.4754131>]

I. INTRODUCTION

Interactions between dihydrogen and metal ions play a central role in hydrogen storage in porous materials, including zeolites, metal-organic frameworks, and nanostructures doped with light elements.^{1–5} Chemists are developing these materials to reversibly bind and store hydrogen in a form that is safer than compressed H_2 gas and which can be used for mobile applications. To optimise these materials it is crucial to understand the nature of the $M^+ \cdots H_2$ interaction. Perhaps the clearest view of the bond between a metal cation and a hydrogen molecule is gained by forming and spectroscopically characterising M^+-H_2 complexes in the gas phase. This has motivated us to characterise a series of M^+-H_2 systems including, Li^+-H_2 and Li^+-D_2 ,^{6,7} Na^+-H_2 and Na^+-D_2 ,^{8,9} Mg^+-H_2 and Mg^+-D_2 ,^{10,11} Al^+-H_2 ,¹² Cr^+-D_2 ,¹³ Mn^+-H_2 ,¹⁴ Zn^+-D_2 ,¹⁵ and Ag^+-H_2 .¹⁶ For several of these systems (Na^+-H_2 ,⁸ Mg^+-H_2 ,¹¹ and Al^+-H_2 ¹²) we have also developed a three-dimensional (3D) potential energy surface (PES) that was used for calculating rovibrational energies.

Among the prospective storage materials are compounds containing boron dopants, which hold promise of high per-

centage weight storage of H_2 and binding energies in a favourable range for absorption and release.^{3,4} In order to guide the rational design of these materials, it is desirable to understand the $B^+ \cdots H_2$ interaction. Previous studies suggest that the $[BH_2]^+$ system possesses two stable structures, the electrostatically bound B^+-H_2 complex (Figure 1(a)), and a covalently bound HBH^+ form (Figure 1(b)).^{17–19} The electrostatic complex has a C_{2v} equilibrium structure, as favoured by the charge-quadrupole interaction between the B^+ cation and the H_2 molecule. Interconversion between the electrostatic complex (Figure 1(a)) and the more stable covalent form (Figure 1(b)) entails surmounting a 252 kJ mol^{-1} barrier associated with a change in electron configuration.¹⁸ Whereas, for B^+-H_2 the valence electron configuration is $2a_1^2 3a_1^2$ (corresponding to ground state B^+ interacting with ground state H_2), the covalently bound HBH^+ molecule has an $2a_1^2 1b_2^2$ electron configuration and correlates with an electronically excited B^+ ion ($2s^1 2p_z^1$ configuration).

There have been several previous experimental studies of the B^++H_2 system, including ion-molecule reactions,²⁰ reactive scattering,^{21–23} and chemiluminescence.²⁴ Most relevant to the current work are thermochemical clustering studies through which the dissociation energy for B^+-H_2 was determined ($D_0 = 1330 \text{ cm}^{-1}$).¹⁹ Corresponding computational investigations have explored the structural properties of B^+-H_2 and interconversion to the covalent BH_2^+ form,^{17,18} and also the anharmonic vibrational frequencies of B^+-H_2 .²⁵

^{a)}Present address: School of Chemistry, The University of Wollongong, Wollongong, Australia.

^{b)}Electronic mail: alexei@classic.chem.msu.su.

^{c)}Electronic mail: jklos@umd.edu.

^{d)}Electronic mail: evanjb@unimelb.edu.au.

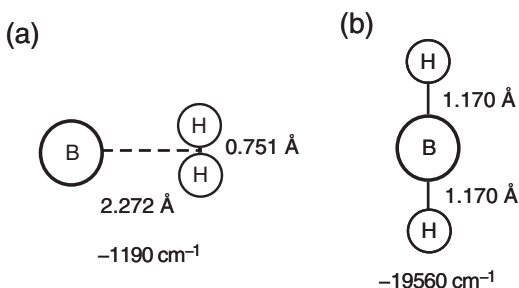


FIG. 1. (a) B^+-H_2 complex; (b) Covalently bound BH_2^+ molecule. Structural parameters are derived at the MP2/aug-cc-pVTZ level and energies with respect to the B^++H_2 limit at the CCSD(T)/aug-cc-pVTZ level. Data are from Ref. 18.

To explore the fundamental $B^+\cdots H_2$ interaction, we have previously recorded the infrared (IR) spectrum of the B^+-H_2 complex in the H-H stretch region.²⁶ The spectrum, in which rotational substructure is clearly resolved, is consistent with a T-shaped equilibrium geometry and a vibrationally averaged intermolecular bond length of 2.26 Å (Figure 1). Unfortunately, the information that could be extracted from the spectrum was limited by the fact that only the $K_a = 1-1$ subband was observed (corresponding to complexes containing ortho H_2). For this reason we could only estimate the ν_{HH} band origin as $3940.6 \pm 1.5 \text{ cm}^{-1}$.

Here we extend the earlier work by presenting an IR spectrum of the corresponding B^+-D_2 isotopologue and a three-dimensional B^++H_2 potential energy surface computed *ab initio* using the coupled cluster CCSD(T) method. The PES is used for variational calculations to derive accurate rovibrational energies for the B^+-H_2 and the B^+-D_2 complexes which are analysed and fitted in a similar fashion to the experimental transition energies, allowing direct comparison between theory and experiment and a direct test of the new PES.

One striking property of B^+-H_2 , compared to other M^+-H_2 complexes studied thus far, is its relatively large vibrational band shift for the H-H stretch vibration ($\Delta\nu_{HH} = -221.5 \text{ cm}^{-1}$) given its relatively low binding energy (1330 cm^{-1}). In comparison, the Li^+-H_2 complex is more strongly bound ($D_0 = 1675 \text{ cm}^{-1}$) yet has a much smaller shift for the H-H stretch mode ($\Delta\nu_{HH} = -107.8 \text{ cm}^{-1}$).

II. POTENTIAL ENERGY SURFACE FOR B^+-H_2

Ab initio calculations for the PES were performed employing electronic structure methods within the MOLPRO 2006 suite.²⁷ The calculations were done with an augmented, correlation-consistent basis set of quadruple-zeta quality (aug-cc-pVQZ) for the hydrogen and B atoms,^{28,29} with the $1s$ orbital on the B atom unfrozen. The basis was augmented with an additional set of $3s3p2d2f1g$ bond functions placed in a mid-distance between B^+ and the H_2 center-of-mass.³⁰ The reference wave function for subsequent coupled-cluster calculations has been obtained at the restricted Hartree-Fock level. The electronic correlation energy is accounted for by using a partially spin-restricted coupled-cluster approach including single and double excitations and

perturbational triple excitations [RCCSD(T)] with explicit correlation of all electrons.^{31,32}

The PES for the B^+-H_2 system is expressed in terms of the Jacobi coordinate system (r, R, θ) , where r denotes the internuclear vector for the H_2 molecule, R is the vector joining the H_2 center-of-mass and the B^+ ion (defining the z axis of the body-fixed frame), and θ is the angle between r and R . The interaction energy was calculated using a supermolecular approach:³³

$$V(r, R, \theta) = E_{B^+-H_2}(r, R, \theta) - E_{B^+}^{DCBS}(r, R, \theta) - E_{H_2}^{DCBS}(r, R, \theta), \quad (1)$$

where $E_{B^+-H_2}(r, R, \theta)$ is the total molecular energy, while $E_{B^+}^{DCBS}(r, R, \theta)$ and $E_{H_2}^{DCBS}(r, R, \theta)$ are the total monomer energies of B^+ or H_2 calculated in the basis set of all bodies – the dimer centered basis set (DCBS). This form for the interaction energy explicitly corrects the basis set superposition error using the standard counter-poise correction scheme.

The PES points were calculated over a grid in which r varies from 1.0 to 2.8 bohr in steps of 0.2 bohr, θ has five values (0° , 22.5° , 45° , 67.5° , and 90°), and R ranges from 3.0 to 40 bohr in 42 steps. *Ab initio* points are available from the authors upon request. The total PES is represented by the sum of the interaction PES, $V(r, R, \theta)$, described above, and the accurate potential for the H_2 diatomic monomer $U(r)$.³⁴

An analytic representation of the three-dimensional PES was obtained using a reproducing kernel Hilbert space (RKHS) method.³⁵ The procedure was the same as described previously for the Mg^+-H_2 system.¹¹

The intermolecular PES for the B^++H_2 interaction, with the H-H bond length fixed to 0.747 Å is shown in Figure 2. The form of the PES is dictated by the electrostatic charge-quadrupole and induction charge-induced-dipole interactions between the B^+ and H_2 components. The minimum in the T-shaped configuration, favoured by both electrostatic and induction interactions, corresponds to $r_{HH} = 0.757 \text{ Å}$, $R = 2.249 \text{ Å}$, and an energy 1557 cm^{-1} below the B^++H_2 asymptote. The linear configuration, where the electrostatic interaction is repulsive and the induction interaction is attractive, represents a saddle point ($r_{HH} = 0.747 \text{ Å}$,

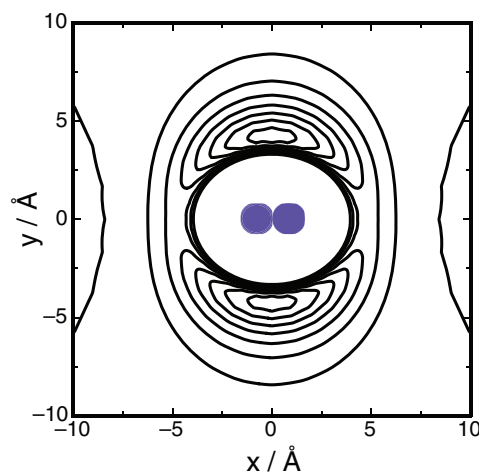


FIG. 2. Contour plot of the B^+-H_2 potential energy surface for a fixed H-H bond length of 0.757 Å . The contour interval is 200 cm^{-1} .

TABLE I. Structural and energetic parameters for equilibrium configurations of the H₂ molecule and B⁺-H₂ electrostatic complex.

	This work	Ref. 18 ^a	Ref. 25 ^b
H₂			
$r_{HH}/\text{\AA}$	0.741	0.7430	0.743
B⁺-H₂			
$r_{HH}/\text{\AA}$	0.757	0.7563	0.756
$R/\text{\AA}$	2.249	2.2546	2.242
D_e/cm^{-1}	1557	1490	1410

^aCCSD(T)/aug-cc-pVTZ calculations.^bCCSD(T)/cc-pVTZ calculations.

$R = 2.514 \text{ \AA}$), corresponding to an energy of -507 cm^{-1} , and a 1050 cm^{-1} barrier to internal rotation. Equilibrium parameters of our PES are compared with other literature *ab initio* results in Table I. Agreement is very good, although our calculations predict slightly larger elongation of H-H bond (0.016 \AA) upon interaction with the B⁺ ion and larger bond energy owing to the use of better saturated basis set.

III. ROVIBRATIONAL CALCULATIONS FOR B⁺-H₂ AND B⁺-D₂

A. Rotational energy levels

The interaction PES described above was used to calculate rovibrational energy levels as described in Ref. 36. Complete details of the calculated rovibrational energy levels for B⁺-H₂ and B⁺-D₂ are provided as supplementary material.³⁷ In brief, the full three-dimensional Hamiltonian expressed in Jacobian coordinates is simplified by separating diabatically the fast H₂ vibrational motion.³⁸ The resulting two-dimensional (2D) problem with effective potentials for each vibrational state of H₂ fragment, $n_{HH} = 0$ and 1, is solved variationally using the basis set constructed from numerical radial functions and analytical symmetry adapted free-rotor spherical functions.³⁶ The latter brings the full Hamiltonian matrix for each total angular momentum quantum number J (excluding nuclear spin) into four blocks (two and three blocks for $J = 0$ and 1, respectively) according to two parity indexes, p_i related to the inversion parity $p = p_i(-1)^J$, and the permutation parity p_j .³⁹ $p_j = +1$ and -1 correspond to complexes containing para H₂ (ortho D₂) and ortho H₂ (para D₂), respectively.

The calculations were performed for each $Jp_i p_j$ block and were converged for the six lowest vibrational energy levels. The levels are classifiable using the nomenclature for an asymmetric top ($J_{K_a K_c}$), and according to the number of quanta in the H₂ stretch mode ($n_{HH} = 0$ or 1) and in the intermolecular stretching and bending vibrational modes (n_s and n_b , respectively).

To test the 2D approach, we also calculated $J = 0$ to 5 energies for the lower vibrational levels with $n_{HH} = 0$ using a full 3D approach. Generally, there is a good agreement between the two methods, both for the rotational energy of the ground vibrational state and also for the energies of the higher intermolecular stretching and bending vibrational states. The main difference is that the 2D approach tends to slightly un-

TABLE II. Comparison of experimental spectroscopic constants for B⁺-H₂ from Dryza *et al.*²⁶ with theoretical constants obtained by fitting the calculated energy levels derived from the PES presented in the current work to a Watson A-reduced Hamiltonian. Units are cm^{-1} unless otherwise indicated.

	Expt. ^a $K_a = 1-1$	Theory 2D $K_a = 0, 1^b$	Theory 3D $K_a = 0, 1^c$
A''	...	72.49(1)	72.35(1)
B''	1.9565(10)	1.9128(5)	1.932(2)
C''	1.8498(10)	1.8124(5)	1.829(2)
\overline{B}''	1.9032(10)	1.8626	1.8805(2)
$\Delta''_J \times 10^4$	2.3(1)	2.45(4)	2.4(5)
$\Delta''_{JK} \times 10^3$...	-8.6(3)	-8.9(9)
A'	...	68.96(1)	
B'	2.0276(10)	1.9830(5)	
C'	1.9045(10)	1.8700(5)	
\overline{B}'	1.9660(10)	1.9265	
$\Delta'_J \times 10^4$	2.3(1)	2.31(5)	
$\Delta'_{JK} \times 10^3$...	-11.2(2)	
ΔA	...	-3.53	
v_{sub}	3936.11(1)		
v_0	3939.64	3957.34	
$rms \times 10^3$	6	7	1
Δv_{HH}	-221.5	-203.8	
ω''_s	346(15)	325(5)	333(66)
ω'_s	363(16)	352(8)	
k''_s	12.0(10)	10.6(03)	11.1(44)
k'_s	13.2(12)	12.4(06)	
$R''_0/\text{\AA}$	2.262	2.287	2.275
$R'_0/\text{\AA}$	2.224	2.247	

^aReference 26.^bFits to $J = 0-10$ levels.^cFits to $J = 0-5$ levels.

derestimate the rotational constants compared to the more accurate 3D approach.

The rotational levels for each rovibrational manifold of B⁺-H₂ and B⁺-D₂ were fitted by the A reduced Watson Hamiltonian to give rotational and centrifugal distortion constants that are directly comparable with corresponding values obtained from analysis of the experimental spectra. The resulting parameters for B⁺-H₂ ($n_{HH} = 0$ and $n_{HH} = 1$ manifolds) and B⁺-D₂ ($n_{DD} = 0$ and $n_{DD} = 1$ manifolds) are reported in Tables II and III, respectively.

The rovibrational calculations provide accurate values for the zero-point vibrational energies and dissociation energies of B⁺-H₂ and B⁺-D₂. The $J = 0$ vibrational ground state level of B⁺-H₂ (para) lies 1254 cm^{-1} below the B⁺+H₂ ($j = 0$) limit, whereas the lowest level of B⁺-H₂ (ortho) ($J = 1$, $K_a = 1$ level) lies 1298 cm^{-1} below the B⁺+H₂ ($j = 1$) limit. The $j = 0$ and $j = 1$ levels correspond to the para and ortho nuclear spin modifications of H₂, which have relative statistical weights of 3:1 and are essentially non-interconverting.

The B⁺-D₂ complex is predicted to be slightly more strongly bound than B⁺-H₂ (by 59 cm^{-1}) due to its lower vibrational zero-point energy associated with the intermolecular stretch and bend vibrational modes. The lowest level of B⁺-D₂ (ortho) lies 1313 cm^{-1} below the B⁺+D₂ ($j = 0$) limit,

TABLE III. Spectroscopic constants for B⁺-D₂ obtained by fitting the D-D stretch band transitions (Fig. 3) and the calculated energy levels derived from the PES to a Watson A-reduced Hamiltonian. Units are cm⁻¹ unless otherwise indicated.

	Expt. $K_a = 0,1$	Theory 2D $K_a = 0,1^a$	Theory 3D $K_a = 0,1^b$
A''		33.664(8)	33.62(1)
B''	1.1410(14)	1.1105(3)	1.122(1)
C''	1.0821(16)	1.0571(3)	1.066(1)
\overline{B}''	1.1116(11)	1.0838(3)	1.094(1)
$\Delta_J'' \times 10^5$	8.0(5)	8.0(3)	8(5)
$\Delta_{JK}'' \times 10^3$	-2.2(14)	-2.7(2)	2.7(7)
A'		32.458(8)	
B'	1.1694(15)	1.1374(3)	
C'	1.1051(16)	1.0800(3)	
\overline{B}'	1.1372(15)	1.1087(3)	
$\Delta_J' \times 10^5$	7.8(7)	7.7(2)	
$\Delta_{JK}' \times 10^3$	-2.8(13)	-3.0(1)	
ΔA	-1.23(1)	-1.22(1)	
ν_0	2839.76(2)	2851.2	
rms $\times 10^3$	7	4	1
$\Delta\nu_{DD}$	-153.8	-142.4	
ω_s''	262(16)	252(9)	256(160)
ω_s'	275(25)	266(7)	
k_s''	11.9(14)	11.0(08)	11.4(142)
k_s'	13.1(24)	12.3(06)	
$R_0''/\text{\AA}$	2.247	2.276	2.265
$R_0'/\text{\AA}$	2.220	2.249	

^aFits to $J = 0-10$ levels.

^bFits to $J = 0-5$ levels.

whereas the lowest level of B⁺-D₂ (para) (the $J = 1$, $K_a = 1$ level) lies 1338 cm⁻¹ below the B⁺+D₂ ($j = 1$) limit.

Assignment of most low lying energy levels is straightforward. However, analysis of several higher intermolecular stretch and bend levels is complicated by Fermi and Coriolis interactions. Specifically, for B⁺-H₂, there is a Coriolis interaction between the $n_{HH} = 0$, $n_b = 1$, $K_a = 1$ levels and adjacent $n_{HH} = 0$, $n_s = 2$, $K_a = 0$ levels. Although the vibrational energy of the $n_{HH} = 0$, $n_b = 1$, $K_a = 1$ state is lower than that of the $n_{HH} = 0$, $\nu_s = 2$, $K_a = 0$ state (543.3 cm⁻¹ compared to 563.4 cm⁻¹), the rotational constant is larger, leading to a crossing of the zero order manifolds at $J'' = 9-10$. Similarly, there are Coriolis interactions between the $n_{HH} = 1$, $n_s = 1$, $K_a = 1$ levels and nearby $n_{HH} = 1$, $n_b = 1$, $K_a = 0$ levels. In this case the vibrational energies are very similar (398.1 cm⁻¹ and 399.2 cm⁻¹) and the zero order manifolds are nearly resonant for $J' = 1$.

The rotational levels of the ν_s , $2\nu_s$, and ν_b manifolds (available as supplementary material³⁷) were also fitted to the expression $E(J) = E_0 + BJ(J+1) - D[J(J+1)]^2$ to give rotational and centrifugal distortion constants that are listed in Table IV.

The rovibrational calculations for B⁺-H₂ enable the ν_{HH} band centre to be defined more precisely than in the original spectroscopic study, in which only the $K_a = 1-1$ sub-band, associated with complexes containing ortho H₂, was observed.²⁶ Fits to the calculated levels allow the separation of $K_a = 0-0$ and $K_a = 1-1$ sub-bands to be predicted (-3.53 cm⁻¹) so that the experimental ν_{HH} band center can be estimated as

TABLE IV. Intermolecular vibrational energies and rotational constants for $K_a = 0$ states of B⁺-H₂ and B⁺-D₂ determined from 2D rovibrational calculations and 3D calculations (in brackets). Units are cm⁻¹.

	E_0''	\overline{B}''	D''	E_0'	\overline{B}'	D'
B ⁺ -H ₂						
GS ($K_a = 0$)	0	1.854	2.4×10^{-4}	0	1.915	2.3×10^{-4}
$\nu_s(K_a = 0)$	304(311)	1.705	2.6×10^{-4}	330	1.774	2.5×10^{-4}
$\nu_b(K_a = 0)$	418(425)	1.822	2.8×10^{-4}	399	1.917	2.7×10^{-4}
$2\nu_s(K_a = 0)$	563(572)	1.539	3.0×10^{-4}	615	1.615	2.8×10^{-4}
B ⁺ -D ₂						
GS ($K_a = 0$)	0	1.0838	8.0×10^{-5}	0	1.1087	7.7×10^{-5}
$\nu_s(K_a = 0)$	239(243)	1.0163	8.7×10^{-5}	253	1.0427	8.4×10^{-5}
$\nu_b(K_a = 0)$	323(325)	1.06630	9.1×10^{-5}	314	1.0998	9.0×10^{-5}
$2\nu_s(K_a = 0)$	454(460)	0.9460	9.3×10^{-5}	480	0.9743	8.9×10^{-5}

3939.64 ± 0.10 cm⁻¹. The fact that the rovibrational calculations for B⁺-D₂ predict the experimentally observed spacing between the $K_a = 0-0$ and $K_a = 1-1$ sub-bands to within 0.01 cm⁻¹ gives credence to the predictions for the B⁺-H₂ sub-band spacing and ν_{HH} band centre.

IV. IR SPECTRUM OF B⁺-D₂

The arrangement for recording IR spectra of mass selected ions has been described previously.^{6,40} The precursor B⁺-D₂ complexes were formed by introducing B⁺ ions from a laser ablated boron nitride rod into a supersonic expansion of D₂ gas. After passing through a skimmer, the B⁺-D₂ ions were mass selected by a primary quadrupole and deflected by 90° into an octopole ion guide where they encountered the counter-propagating output of the tuneable IR light-source (Continuum Mirage 3000, line-width 0.017 cm⁻¹). The B⁺ fragment ions resulting from resonant absorption of an IR photon were mass selected by a second quadrupole mass filter and finally sensed using a micro-channel plate coupled to a scintillator and a photomultiplier tube. Typically, populations of charged complexes formed in the supersonic expansion ion source have a rotational temperature of 30–40 K. Transition wavenumbers are corrected for the small Doppler shift arising from the ions' kinetic energy (10 eV) in the octopole guide where they overlap with the IR radiation.

The IR spectrum of B⁺-D₂ in the D-D stretch (2800–2880 cm⁻¹) is shown in Figure 3. The form of the spectrum, which displays three overlapping $K_a = 0-0$, 1-1, and 2-2 sub-bands, accords with expectations for a T-shaped complex and is consistent with the previously recorded infrared spectrum of B⁺-H₂.²⁶ Excitation of the H-H or D-D sub-unit leads to a transition dipole moment lying along the principle axis of the molecule (intermolecular bond), and a parallel IR transition. Asymmetry doublets are clearly resolved for the $K_a = 1-1$ sub-band (see enlargement of the Q-branch region in Figure 3), but not for the $K_a = 2-2$ sub-band for which the spacing is predicted to be much smaller.

Altogether, in the B⁺-D₂ spectrum, 23 lines were identified for the $K_a = 0-0$ sub-band, 30 lines for the $K_a = 1-1$ sub-band, and 20 lines for the $K_a = 2-2$ sub-band. The $K_a = 0-0$ and $K_a = 2-2$ transitions overlap at higher J in the R-branch. The line wavenumbers were fitted to a

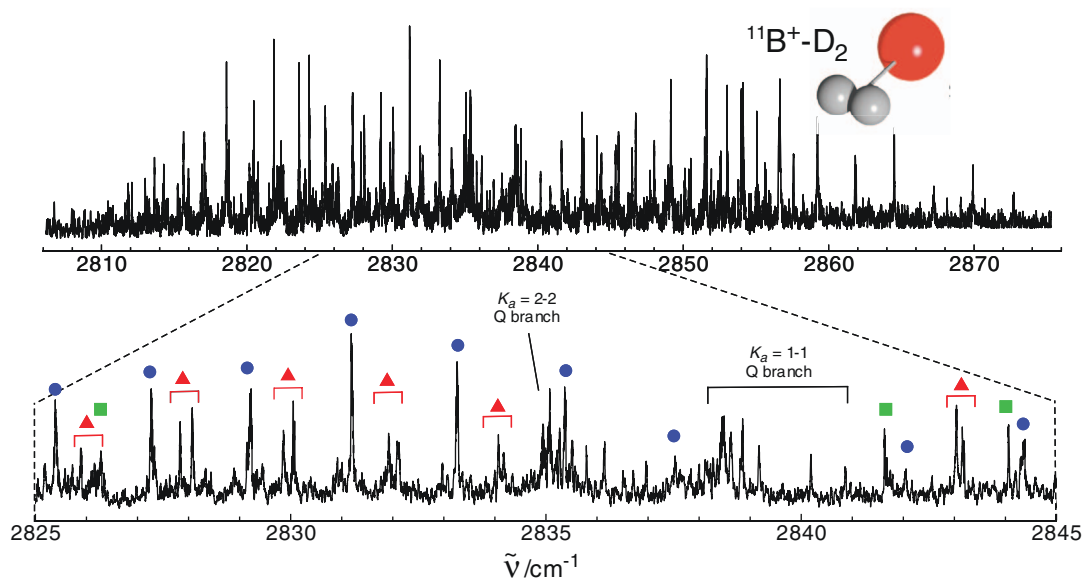


FIG. 3. IR spectrum of the B^+-D_2 complex in the D-D stretch region (upper), along with an expanded view of the Q branch region (lower). $K_a = 0-0$ transitions are indicated by filled circles (\bullet), $K_a = 1-1$ transitions by filled triangles (\blacktriangle) and $K_a = 2-2$ transitions by filled squares (\blacksquare).

Watson A -reduced Hamiltonian for an asymmetric rotor,⁴¹ yielding the band centre for the ν_{DD} transition, ground and excited state B and C rotational constants, and Δ_J and Δ_{JK} centrifugal distortion terms. For fitting individual sub-bands, both A'' and A' were constrained to 29.907 cm^{-1} , the ground state rotational constant of the bare D_2 molecule.⁴² When two or more sub-bands were fitted together, A'' was constrained to 29.907 cm^{-1} whereas A' was allowed to vary. It is worth noting that values of the other constants are relatively insensitive to substantial variations in A'' or A' . Spectroscopic constants obtained from the fits are presented in Table III. The supplementary material³⁷ includes a complete list of the observed transitions, assignments in terms of a near prolate asymmetric rotor model, and deviations from the line positions predicted using the parameters in Table III.

V. DISCUSSION

Here we consider the nature of the $B^+\cdots H_2$ interaction in light of the IR spectra of B^+-H_2 and B^+-D_2 and the new B^++H_2 PES and rovibrational calculations. The B^+-H_2 and B^+-D_2 spectra, with their prominent $\Delta K_a = 0$ sub-bands are qualitatively consistent with the *ab initio* PES, which features a pronounced minimum in the T-shaped configuration lying 1050 cm^{-1} below the linear configuration (Fig. 2). The vibrationally averaged intermolecular bond length for B^+-D_2 deduced from the ground state rotational constant (\bar{B}'') is 2.247 \AA , slightly less than for B^+-H_2 (2.262 \AA), reflecting the reduced amplitude of the zero-point stretching motion resulting from the larger mass of the D_2 sub-unit.

Despite the substantial barrier for internal rotation the bending wave function has significant amplitude in configurations well away from the T-shaped minimum, a consequence of the low mass of the H_2 (D_2) sub-unit. The IR spectrum provides subtle evidence for the large amplitude bending vibrations of B^+-D_2 and B^+-H_2 , particularly through the ex-

aggerated spacing of the $K_a = 1-1$ asymmetry doublets and large differences in the B and C rotational constants. As noted for other M^+-H_2 complexes, the value of the A rotational constant derived from B and C constants, assuming a zero inertial defect as expected for a rigid, planar molecule ($1/A = 1/C - 1/B$), is inconsistent with a reasonable H-H bond length. For example, the H-H and D-D bond lengths deduced from the rotational constants listed in Tables II and III are 0.99 \AA and 0.89 \AA , respectively. Obviously, the H-H and D-D bond lengths should be very similar and much smaller – the *ab initio* equilibrium separation is around 0.76 \AA . In fact, the complexes are floppy and undergo large amplitude vibrational excursions along the bend coordinates leading to a non-zero inertial defect. These large amplitude motions are accounted for explicitly in the rovibrational calculations.

A. Vibrational band shifts

A characteristic feature of the M^+-H_2 complexes is that interaction with the metal cation leads to a reduction in vibrational frequency for the H_2 and D_2 sub-units and increase in the H-H and D-D bond lengths.^{16,43} The ν_{DD} band origin for B^+-D_2 occurs at 2839.75 cm^{-1} , corresponding to a shift of -153.8 cm^{-1} with respect to the $Q_1(0)$ transition of the free D_2 molecule. The relative shift of the D-D stretch band ($\Delta\nu_{DD}/\nu_{DD} = -0.053$) is almost identical to the corresponding relative shift for the H-H stretch transition of B^+-H_2 ($\Delta\nu_{HH}/\nu_{HH} = -0.051$).²⁶ The vibrational shifts for B^+-H_2 and B^+-D_2 are larger than for other M^+-H_2 and M^+-D_2 complexes having comparable dissociation energies. For example, the shifts for B^+-H_2 and B^+-D_2 are nearly double those for Li^+-H_2 and Li^+-D_2 (for both of which $\Delta\nu/\nu = -0.026$), despite the fact that the dissociation energies for Li^+-H_2 and Li^+-D_2 are around 300 cm^{-1} higher than for B^+-H_2 and B^+-D_2 . This implies that the

vibrational redshift is not entirely determined by long range electrostatic and induction interactions, a significant implication given that the magnitude of the vibrational redshift is sometimes used to infer the H₂ binding energy in porous hydrogen storage materials.⁴³ The same exceptions have been noted in Ref. 25.

Data for other M⁺-H₂ and M⁺-D₂ complexes suggest that the electronic structure of the metal cation influences the vibrational shift. Complexes containing metal cations with s⁰, s¹ and s², and d⁵ and d¹⁰ valence electronic structures each display different relationships between the vibrational band shift and dissociation energy.^{15,16} In the case of B⁺-H₂, a natural bond orbital analysis suggests that the pronounced lengthening and softening of the H-H bond and resulting large $\Delta\nu_{HH}$ shift are associated with the transfer of electron density from the H₂ σ_g bonding orbital to the opposite side of the B⁺ cation, facilitated through hybridisation of the B⁺ valence 2s orbital with the low lying 2p_z orbital.²⁶

The relatively large vibrational redshifts for B⁺-H₂ and B⁺-D₂, are also reflected in a substantial lengthening of the H-H and D-D bonds accompanying formation of the complexes (by 0.016 Å), larger than for comparable complexes, including Li⁺-H₂ (0.010 Å), Na⁺-H₂ (0.005 Å) and Mg⁺-H₂ (0.008 Å).

B. Intermolecular vibrational modes

The B⁺-H₂ and B⁺-D₂ IR spectra currently provide little direct information on the intermolecular bend (ν_b) or stretch (ν_s) vibrational modes and resort must be made to theory for their frequencies. Calculated frequencies and rotational constants for ν_s , $2\nu_s$, and ν_b , derived from the 2D and 3D rovibrational calculations are reported in Table IV. Generally, the assignments for the calculated vibrational levels are compatible with the rotational constants for the manifolds. For example, the rotational constants for the ν_s and $2\nu_s$ levels are less than for the ground state, due to increases in the vibrationally averaged intermolecular separation. The intermolecular bend mode, on the other hand, has a very similar rotational constant to the ground state, indicating that, as is apparent from Figure 2, the radial separation does not change markedly along the bending coordinate. Note however, that the centrifugal distortion constants for the ν_b states are systematically larger than the ground state, reflecting the fact that the intermolecular interaction becomes weaker as the system moves towards the linear configuration.

Although we do not measure ν_s directly, estimates for the harmonic intermolecular stretch frequency (ω_s) derived from the rotational constant and centrifugal distortion constant (\bar{B} and Δ_J) by treating the system as a pseudo-diatomic are around 10% larger than the stretching frequencies predicted through the rovibrational calculations (Tables II and III).

Vibrational excitation of the diatomic H₂ or D₂ sub-unit leads to a contraction of the intermolecular bond (by 0.038 and 0.027 Å for B⁺-H₂ and B⁺-D₂, respectively) and an increase in the predicted intermolecular stretch frequency (304 to 330 cm⁻¹ for B⁺-H₂ and 239 to 253 cm⁻¹ for B⁺-D₂). The shortening and stiffening of the intermolecular bond, which is

quantitatively reproduced by theory, is in line with increases of the vibrationally averaged polarisability and quadrupole moment of the H₂ or D₂ molecule accompanying vibrational excitation of the diatomic molecule.

Although the ν_s mode increases in frequency upon excitation of the diatomic sub-unit, somewhat surprisingly, the intermolecular bending mode decreases in frequency (Table IV). This reduction has neither been predicted nor observed for other M⁺-H₂ complexes, and is possibly connected with the fact that as the H-H bond is stretched the angular potential progressively becomes more isotropic. Indeed, analysis of the PES shows that when r exceeds ~ 1.1 Å, the linear HHB⁺ structure actually becomes favoured over the T-shaped structure.

C. Assessing the B⁺+H₂ potential energy surface

One of the main goals of this work is to develop a reliable PES for the B⁺+H₂ interaction, capable of describing the properties of the B⁺-H₂ and B⁺-D₂ complexes. Points of contact between theory and experiment include the dissociation energy and the measured and calculated spectroscopic parameters listed in Tables II and III.

The PES does a good job of predicting the binding energy of B⁺-H₂, with a calculated dissociation energy of 1254 cm⁻¹ for B⁺-H₂ (para) and 1298 cm⁻¹ for B⁺-H₂ (ortho) reproducing the measured value ($D_0 = 1330 \pm 70$ cm⁻¹; Ref. 19) very well.

The measured rotational and centrifugal distortion constants for B⁺-H₂ and B⁺-D₂ are also reproduced quite well by the 2D and 3D rovibrational calculations. The 3D calculations underestimate B'' by 1%–2%, corresponding to an overestimation of the vibrationally averaged intermolecular bond length by 0.01–0.02 Å, perhaps an indication that the PES slightly underestimates the strength of the intermolecular interaction. Furthermore, the 2D rovibrational calculations correctly predict the magnitude of contraction and stiffening of the intermolecular bond following excitation of the diatomic sub-unit. Furthermore, the calculations predict the spacings between the $K_a = 0-0$, 1-1, and 2-2 sub-band origins for B⁺-D₂ to within 0.01 cm⁻¹.

Perhaps the largest discrepancies are for the vibrational band shifts of B⁺-H₂ and B⁺-D₂, which the new PES and 2D rovibrational calculations predict to be –204 and –142 cm⁻¹, underestimating the experimental shifts (–224 and –154 cm⁻¹) by around 8% in both cases.

The same discrepancy was found in previous variational calculations for other M⁺-H₂ complexes.^{8,11,12} Although inaccuracy of the PES cannot be ruled out as a possible origin, we tend to attribute it to the use of 2D approximation, which expresses the 2D intermolecular PES as an average over the vibrational motion of the unperturbed H₂ molecule in the $n_{HH} = 0$ and $n_{HH} = 1$ states. This approach becomes less accurate for systems in which the interaction with the metal cation significantly affects the H-H potential. One therefore finds better agreement between the 2D and 3D results for complexes with smaller distortion of the H₂ fragment. It is difficult to quantify the defect of 2D approximation for the $n_{HH} = 1$ levels because they are not amenable to 3D

variational calculations as they are metastable with respect to vibrational predissociation.

De Silva *et al.* have performed *ab initio* calculations at the CCSD(T)/cc-pVTZ level for the B^+-H_2 complex, using a vibrational self consistent field (VSCF) method to account for vibrational anharmonicity.²⁵ Generally, the VSCF anharmonic frequencies are much closer than the harmonic frequencies to the values predicted from our rovibrational calculations. The predicted redshift for ν_{HH} is -202 cm^{-1} (similar to our prediction of -204 cm^{-1}), whereas the VSCF frequency for ν_s is 306 cm^{-1} , again similar to our prediction (311 cm^{-1} from the 3D calculations). On the other hand, the VSCF frequency for ν_b (480 cm^{-1}) is somewhat larger than our value (425 cm^{-1} from the 3D calculations). The same trends hold for other M^+-H_2 complexes considered in Ref. 25. Potentially the VSCF approach, which relies on derivatives of the potential energy at the equilibrium configuration, may not adequately describe the large amplitude bending mode that corresponds to a frustrated internal rotation.

The zero-point corrected dissociation energy, 1116 cm^{-1} , is around 11% less than our value (1254 cm^{-1}) and 16% less than the measured value. Ultimately, direct spectroscopic measurements of the ν_s and ν_b modes would provide firmer tests of our PES and rovibrational calculations and the VSCF calculations.

VI. CONCLUDING REMARKS

The experimental and theoretical data confirm that the B^+-H_2 and B^+-D_2 complexes essentially consist of a B^+ cation attached to a slightly perturbed H_2 or D_2 molecule, notwithstanding the fact that the predicted lowest energy form of the $[BH_2]^+$ system is the linear, covalently bound HBH^+ molecule. The main evidence for the weak nature of the $B^+\cdots H_2$ bond is that the H-H and D-D stretch bands of B^+-H_2 and B^+-D_2 are only mildly shifted from the vibrational transitions of the free H_2 and D_2 molecules (by -221.5 and -153.8 cm^{-1} , respectively) and that the spectra are consistent with T-shaped equilibrium structures, favoured by the electrostatic charge-quadrupole interaction, with intermolecular separations of approximately 2.25 \AA . Both experiment and theory demonstrate the importance of large amplitude motions in the intermolecular stretch and bend modes in influencing the measured spectroscopic constants.

The new B^++H_2 PES provides a good description of B^+-H_2 and B^+-D_2 . The predicted dissociation energy of B^+-H_2 (para) is 1254 cm^{-1} , agreeing with the experimental value ($D_0 = 1330 \pm 70\text{ cm}^{-1}$; Ref. 19). The predicted dissociation energy for B^+-D_2 (ortho) is slightly larger (1313 cm^{-1}) due to its lower zero-point energy. The calculations predict key features of the B^+-H_2 and B^+-D_2 complexes, including the shortening of the intermolecular bond following vibrational excitation of the diatomic sub-unit (by 0.038 and 0.027 \AA , respectively), and the separation of the sub-bands in the B^+-D_2 spectrum. The calculations underestimate the rotational constants by around 1%–2%, and underestimate the band shifts for the H-H and D-D transitions by 7%–8%.

ACKNOWLEDGMENTS

This research was supported under the Australian Research Council's Discovery Project funding scheme (Project Nos. DP0986980, DP110100312, and DP120100100). J.K. acknowledges financial support from the U.S. National Science Foundation (Grant No. CHE-0848110) to Professor M. H. Alexander. Electronic structure calculations were performed on the OIT High Performance Computing Cluster (HPCC) of the University of Maryland.

- ¹M. Felderhoff, C. Weidenthaler, R. von Helmolt, and U. Eberle, *Phys. Chem. Chem. Phys.* **9**, 2643 (2007).
- ²M. Dinca and J. Long, *Angew. Chem., Int. Ed. Engl.* **47**, 6766 (2008).
- ³L. Firlej, B. Kuchta, C. Wexler, and P. Pfeifer, *Adsorption* **15**, 312 (2009).
- ⁴Y. Liu, C. Brown, J. Blackburn, D. Neumann, T. Gennett, L. Simpson, P. Parilla, A. Dillon, and M. Heben, *J. Alloys Compd.* **446-447**, 368 (2007).
- ⁵S. Banerjee, S. Murad, and I. K. Puri, *Proc. IEEE* **94**, 1806 (2006).
- ⁶C. D. Thompson, C. Emmeluth, B. L. J. Poad, G. H. Weddle, and E. J. Bieske, *J. Chem. Phys.* **125**, 044310 (2006).
- ⁷C. Emmeluth, B. L. J. Poad, C. D. Thompson, G. H. Weddle, and E. J. Bieske, *J. Chem. Phys.* **126**, 204309 (2007).
- ⁸B. L. J. Poad, P. J. Wearne, E. J. Bieske, A. A. Buchachenko, D. I. G. Bennett, J. Kłos, and M. H. Alexander, *J. Chem. Phys.* **129**, 184306 (2008).
- ⁹B. L. J. Poad, V. Dryza, J. Kłos, A. A. Buchachenko, and E. J. Bieske, *J. Chem. Phys.* **134**, 214302 (2011).
- ¹⁰V. Dryza, B. L. J. Poad, and E. J. Bieske, *J. Phys. Chem. A* **113**, 199 (2009).
- ¹¹V. Dryza, E. J. Bieske, A. A. Buchachenko, and J. Kłos, *J. Chem. Phys.* **134**, 044310 (2011).
- ¹²C. Emmeluth, B. L. J. Poad, C. D. Thompson, G. H. Weddle, E. J. Bieske, A. A. Buchachenko, T. A. Grinev, and J. Kłos, *J. Chem. Phys.* **127**, 164310 (2007).
- ¹³V. Dryza and E. J. Bieske, *J. Chem. Phys.* **131**, 164303 (2009).
- ¹⁴V. Dryza, B. L. J. Poad, and E. J. Bieske, *J. Phys. Chem. A* **113**, 6044 (2009).
- ¹⁵V. Dryza and E. J. Bieske, *J. Chem. Phys.* **131**, 224304 (2009).
- ¹⁶V. Dryza and E. J. Bieske, *J. Phys. Chem. Lett.* **2**, 719 (2011).
- ¹⁷J. Nichols, M. Gutowski, S. J. Cole, and J. Simons, *J. Phys. Chem.* **96**, 644 (1992).
- ¹⁸S. Sharp and G. Gellene, *J. Am. Chem. Soc.* **120**, 7585 (1998).
- ¹⁹P. Kemper, J. Bushnell, P. Weis, and M. Bowers, *J. Am. Chem. Soc.* **120**, 7577 (1998).
- ²⁰C. H. DePuy, R. Gareyev, J. Hankin, G. E. Davico, and R. Damrauer, *J. Am. Chem. Soc.* **119**, 427 (1997).
- ²¹B. Friedrich and Z. Herman, *Chem. Phys.* **69**, 433 (1982).
- ²²K. Lin, H. P. Watkins, R. J. Cotter, and W. S. Koski, *J. Chem. Phys.* **60**, 5134 (1974).
- ²³N. A. Sondergaard, I. Sauters, A. C. Jones, J. J. Kaufman, and W. S. Koski, *J. Chem. Phys.* **71**, 2229 (1979).
- ²⁴C. Ottinger and J. Reichmuth, *J. Chem. Phys.* **74**, 928 (1981).
- ²⁵N. De Silva, B. Njegic, and M. S. Gordon, *J. Phys. Chem. A* **115**, 3272 (2011).
- ²⁶V. Dryza, B. L. J. Poad, and E. J. Bieske, *J. Am. Chem. Soc.* **130**, 12986 (2008).
- ²⁷H.-J. Werner, P. J. Knowles, R. Lindh, F. R. Manby, M. Schütz *et al.*, MOLPRO, version 2006.1, a package of *ab initio* programs, 2006, see <http://www.molpro.net/>.
- ²⁸R. A. Kendall, T. H. Dunning, Jr., and R. J. Harrison, *J. Chem. Phys.* **96**, 6796 (1992).
- ²⁹D. E. Woon and T. H. Dunning, Jr., *J. Chem. Phys.* **100**, 2975 (1994).
- ³⁰S. M. Cybulski and R. R. Toczylowski, *J. Chem. Phys.* **111**, 10520 (1999).
- ³¹P. J. Knowles, C. Hampel, and H.-J. Werner, *J. Chem. Phys.* **99**, 5219 (1993).
- ³²P. J. Knowles, C. Hampel, and H.-J. Werner, *J. Chem. Phys.* **112**, E3106 (2000).
- ³³M. H. Alexander, *J. Chem. Phys.* **108**, 4467 (1998).
- ³⁴W. Cencek, private communication (2011).
- ³⁵T. S. Ho and H. Rabitz, *J. Chem. Phys.* **104**, 2584 (1996).
- ³⁶A. A. Buchachenko, T. A. Grinev, J. Kłos, E. J. Bieske, M. M. Szczyński, and G. Chałasiński, *J. Chem. Phys.* **119**, 12931 (2003).

- ³⁷See supplementary material at <http://dx.doi.org/10.1063/1.4754131> for calculated B⁺-H₂ and B⁺-D₂ rovibrational energy levels and for measured transition energies of B⁺-D₂.
- ³⁸G. Delgado-Barrio and J. A. Beswick, *Structure and Dynamics of Non-rigid Molecular Systems* (Kluwer, Dordrecht, 1994), p. 203.
- ³⁹B. P. Reid, K. C. Janda, and N. Halberstadt, *J. Phys. Chem.* **92**, 587 (1988).
- ⁴⁰D. A. Wild and E. J. Bieske, *Int. Rev. Phys. Chem.* **22**, 129 (2003).
- ⁴¹J. K. G. Watson, *J. Chem. Phys.* **46**, 1935 (1967).
- ⁴²K. P. Huber and G. Herzberg, *Molecular Spectra and Molecular Structure IV. Constants of Diatomic Molecules* (van Nostrand Reinhold, New York, 1979).
- ⁴³J. G. Vitillo, A. Damin, A. Zecchina, and G. Ricchiardi, *J. Chem. Phys.* **122**, 114311 (2005).